A Comparative Analysis of DeepDentalNet: An AI-Assisted Voxel-Based Segmentation of Sinus, Mandibular Canal, and Missing Tooth Regions in CBCT-Based Implant Planning

Rajashree Nambiar
Faculty of Engineering and Technology, JAIN (Deemed to be University), Bengaluru, India | Department of Robotics & AI, NMAM Institute of Technology (NMAMIT), Nitte (Deemed to be University), Nitte, Karnataka, India
raji24oct@gmail.com (corresponding author)

Raghu Nanjundegowda
Department of Electrical and Electronics Engineering, Faculty of Engineering and Technology, JAIN (Deemed to be University), Bengaluru, India
raghu1987n@gmail.com

Received: 17 August 2025 | Revised: 24 September 2025 and 9 October 2025 | Accepted: 12 October 2025

 DOI: https://doi.org/10.48084/etasr.14124

ABSTRACT

Dental implant planning is a critical aspect of restorative dentistry that requires precise preoperative assessment of bone structures to ensure optimal implant placement and long-term success. Traditional methods rely heavily on manual interpretation of Cone Beam Computed Tomography (CBCT) scans and are sometimes time-intensive and susceptible to inter-observer variability. In this study, a deep learning-based approach using a 3D UNET model with residual connections is proposed to automate the segmentation of key anatomical structures, including the missing tooth bone region, sinus, and mandibular canal. The proposed model was trained using a combination of Dice Loss and Binary Cross-Entropy (BCE) Loss, ensuring accurate segmentation. The model achieved Dice Similarity Coefficients (DSC) of 94.1% for the missing tooth region, 91.8% for the maxillary sinus, and 92.5% for the mandibular canal, demonstrating high segmentation accuracy. Additionally, bone length and breadth were measured automatically. The proposed AI-driven methodology streamlines implant planning, enhances efficiency, and reduces manual workload, offering a promising tool for clinical applications.

Keywords-artificial intelligence; deep learning; dental imaging; residual connection; semantic segmentation; 3D UNET

I. INTRODUCTION

Dental implants have long been a popular therapeutic choice for restoring either whole, partial, or single tooth edentulism. The success of implant placement is highly dependent on precise preoperative planning, which ensures optimal positioning and minimizes surgical risks. Traditionally, implant placement has been performed in healed extraction sites. However, immediate implant placement following tooth extraction has gained popularity due to its ability to reduce the number of surgical interventions and shorten the overall treatment duration. Research indicates that implants placed in fresh extraction sockets demonstrate comparable survival rates to those placed in healed sites, with studies reporting success rates exceeding 90% within the first year of placement [1]. While conventional panoramic and intraoral radiographs provide a general overview of jaw structures, they lack the precision required for detailed implant planning. Cone Beam Computed Tomography (CBCT) has emerged as a superior alternative, providing three-dimensional (3D) high-resolution, reduced radiation exposure, quicker scan periods visualization of bone structures as compared to traditional Computed Tomography (CT) [2]. CBCT plays a pivotal role in evaluating bone quality, determining implant dimensions, and predicting the need for adjunctive procedures such as guided bone regeneration, ridge splitting, or sinus augmentation [3].

Despite advancements in imaging technology, implant planning remains highly dependent on the clinician's expertise in interpreting CBCT scans. Recent developments in Artificial Intelligence (AI) and Deep Learning (DL) have introduced the potential for automated analysis of CBCT images, enhancing

diagnostic accuracy and treatment planning. DL models can assist in segmenting anatomical structures, assessing bone density, and predicting optimal implant placement, reducing human error and improving overall treatment outcomes [4].

Despite ongoing advancements in the field of medical image computing, fully automated segmentation of teeth and alveolar bones remains both a technical and practical challenge, with no clinically deployable system currently available. Over the past decade, various methods have been developed to extract hand-crafted features for tooth segmentation, including level set models, graph cut algorithms, and template fitting techniques [5]. However, these traditional approaches are highly sensitive to the complexities of dental CBCT images. The use of Convolutional Neural Networks (CNNs) has demonstrated significant potential across multiple domains due to their ability to learn representative and task-specific features directly from large-scale datasets [6]. Inspired by their success in medical image analysis and computer vision, researchers have explored Deep Neural Networks (DNNs) for segmenting teeth and alveolar bone structures [7, 8]. However, these methods still face several limitations that hinder their full automation and clinical applicability.

The first challenge lies in the complexity of segmenting individual teeth, segmenting the alveolar bone, and localizing the dental Region of Interest (RoI). Instead of offering an end-to-end solution, most of the current research concentrates on just one of these processes, such as alveolar bone segmentation or tooth segmentation inside a predetermined RoI. Secondly, handling complex clinical cases remains difficult, particularly when dealing with CBCT scans of patients exhibiting anatomical variations, missing teeth, misalignment, or artifacts from metal restorations. Lastly, most of the prior research has been conducted on relatively small datasets, often consisting of only CBCT scans, which limits the generalizability and applicability of these methods across different imaging protocols and diverse patient demographics.

DL techniques provide an effective solution by accurately segmenting the bone regions associated with missing teeth in CBCT scans, thereby improving prediction accuracy [9]. This study introduces a DL-based methodology aimed at optimizing dental implant planning. One of the two U-Net-based DL models created dealed with maxillary bone segmentation and sinus in CBCT scans and another with segmenting the mandibular canal and tooth bone.

II. PROPOSED METHODOLOGY

A. Dataset

The dataset comprised 75 anonymized CBCT scans obtained from individuals aged from 18 to 70 years, representing both maxillary and mandibular regions with a nearly balanced gender distribution (52% female and 48% male). Scans that exhibited motion artifacts or poor image quality were excluded from the study. The dataset used in this study was obtained directly from a collaborating dental clinic and contains patient-specific radiographic images. Due to confidentiality agreements and patient privacy concerns, the dataset cannot be made publicly available. However, access may be granted upon reasonable request and with appropriate ethical approvals. Each image volume was reconstructed with a voxel dimension of 1 mm³ and a slice thickness of one voxel, providing complete coverage across the coronal, sagittal, and axial planes. Sample dataset images are shown in Fig. 1.

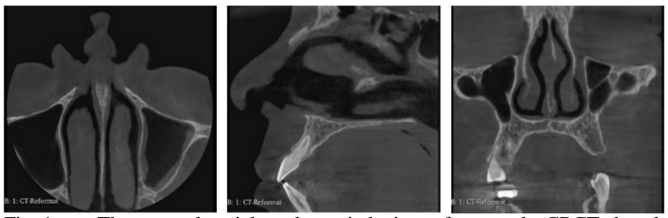

Fig. 1. The coronal, axial, and saggital view of a sample CBCT dental image.

B. Annotations

A skilled professional with more than 10 years of experience in dental implant design helped in manually annotating each patient's CBCT pictures using the 3D Slicer (5.8.0) program in order to provide ground truth labels. 3D offers advanced features for annotation, image fusion, and 3D model reconstruction from DICOM data. The software also includes transformation capabilities, ensuring standardization of head positioning in both anteroposterior and sagittal views. A systematic division of each jaw into anterior and posterior portions allowed it to be classified as either the mandible or the maxilla. The presence of any missing teeth and important anatomical features such sinuses, canals, and alveolar bone fossae were meticulously recorded. Manual measurements of bone thickness and height were made in edentulous regions while taking anatomical limitations into consideration and according to normal implant planning procedures. Figure 2 shows the 3D Slicer image view in both 2D and 3D.

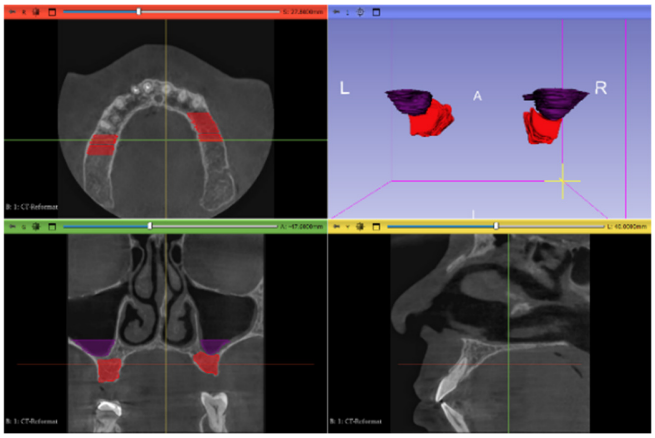

Fig. 2. 3D slicer view of a CBCT image.

C. 3DUNET Model with Residual Connections

To perform segmentation, a 3D UNET architecture, as shown in Figure 3, with residual connections was employed. The standard 3D UNET is widely used for medical image segmentation due to its encoder-decoder structure, which captures both high-level and fine-grained details [10]. At the bottleneck layer, a 3D convolution (kernel 3×3×3) is used,

followed by batch normalization and a dropout layer (rate = 0.3) to prevent overfitting. The decoder path mirrors the encoder but replaces max pooling with transposed convolutions (stride 2) for up-sampling. Skip connections between the corresponding encoder and decoder layers help preserve spatial information, crucial for accurate boundary segmentation. The final output layer consists of a 1×1×1 convolutional layer with a sigmoid activation function, generating a binary segmentation mask.

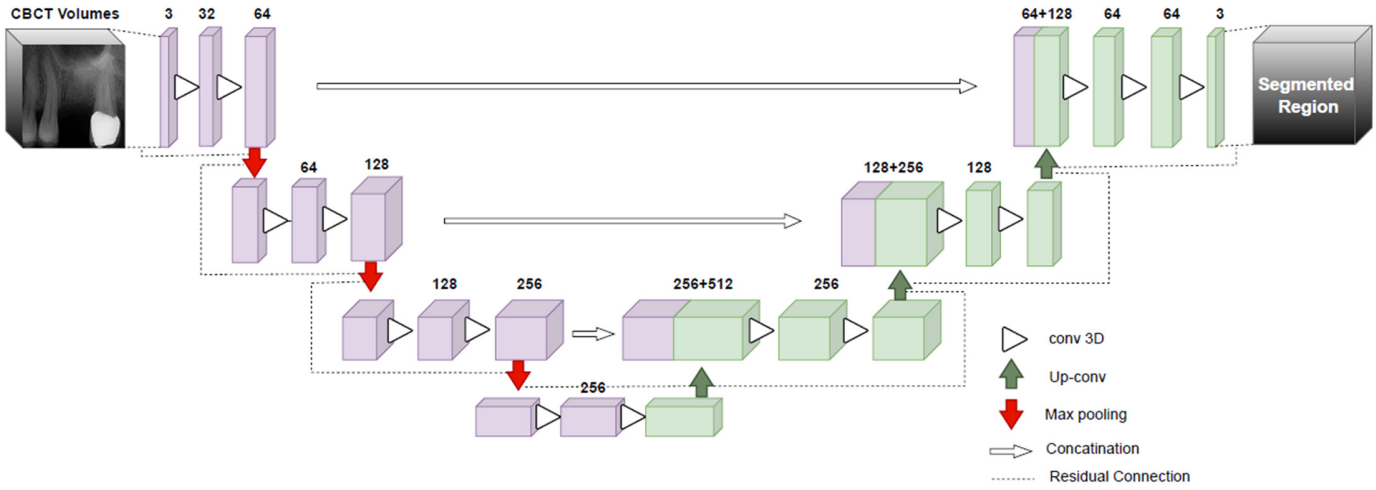

Fig. 3. Proposed 3D UNET with residual connections.

D. 3DUNET Model with Residual Connections

After segmenting the missing tooth bone region, sinus, and mandibular canal in CBCT images, the next crucial step is to determine bone size to aid in dental implant planning. The bone size measurement involves two primary aspects: (1) calculating the available bone length, ensuring a 2 mm safety margin from critical anatomical structures, and (2) measuring the bone breadth at three different depths from the jaw base at 3 mm intervals. These measurements are essential for evaluating whether the bone volume is sufficient to support an implant and if additional surgical interventions like bone grafting or ridge augmentation are necessary. This methodology outlines the structured approach to measuring bone length and breadth from 3D segmented CBCT images, ensuring clinical accuracy and reproducibility.

1) Bone Length Measurement with a 2 mm Safety Margin

Bone length is one of the most critical parameters in dental implant planning, as it defines the maximum permissible implant height while ensuring that the implant does not interfere with essential anatomical structures. In maxillary cases, the implant site must maintain a minimum clearance of 2 mm from the maxillary sinus to prevent sinus membrane perforation, which can lead to complications such as sinusitis or implant failure. Similarly, in mandibular cases, the implant should remain at least 2 mm away from the mandibular canal, which houses the inferior alveolar nerve. Failure to maintain this margin can result in nerve damage, leading to sensory disturbances or permanent numbness in the lower lip and chin. By ensuring these safety margins, the implant remains in a safe zone, reducing the risk of complications while maximizing available bone for support.

2) Steps for Bone Length Calculation

The total available bone length is calculated by measuring the vertical distance from the jaw base to the upper boundary of the implant region, while ensuring that the 2 mm safety margin from critical structures is maintained. The first step in bone length measurement involves identifying the uppermost and lowermost boundaries of the segmented bone region in the Z-axis (vertical direction). The lowest Z-coordinate (Z_{min}) represents the jaw base, which serves as the reference for bone height measurements. The highest Z-coordinate (Z_{max}) defines the top boundary of the implantable bone region, providing the initial estimate of available bone height. Once the total bone height is estimated, the next step involves measuring the distance to the closest anatomical constraints, which may limit the available implantable length. These constraints differ based on the jaw region: In maxillary implants, the distance d_{sinus} is calculated from the top boundary of the implant site (Z_{max}) to the maxillary sinus floor. In mandibular implants, the distance $d_{mandibular\_canal}$ is measured from Z_{max} to the superior border of the mandibular canal as in (1) and (2).

3) Applying the Safety Margin

If the distance to the sinus or mandibular canal is less than 2 mm, the available implantable bone length must be adjusted accordingly. This ensures that the implant does not encroach on these vital structures.

If $d_{sinus} < 2$ mm, the final bone length is calculated by:

$$L = Z_{max} - Z_{min} - \max(2, d_{sinus}) \quad (1)$$

If $d_{mandibular_canal} < 2$mm, the final bone length is computed by:

$$L = Z_{max} - Z_{min} - \max(2, d_{mandibular\_canal}) \quad (2)$$

These corrections ensure that the implantable length remains within safe clinical limits while maximizing available bone utilization. If the adjusted bone length is significantly reduced, alternative implant planning strategies might be needed. If the measured bone length is less than 8 mm, implant placement may not be feasible without additional surgical interventions.

III. RESULTS AND DISCUSSION

A. Qualitative Evaluation of Segmentation Results

The effectiveness of the proposed 3D UNET model with residual connections was evaluated on a dataset of 75 dental CBCT images. The segmentation results were visually compared against expert-annotated ground truth images. Figure 4(a) and 4(b) illustrate the manually annotated regions for the missing tooth and critical anatomical structures such as the sinus and mandibular canal. Figures 4(c) and 4(d) present the corresponding segmentation outputs generated by the model.

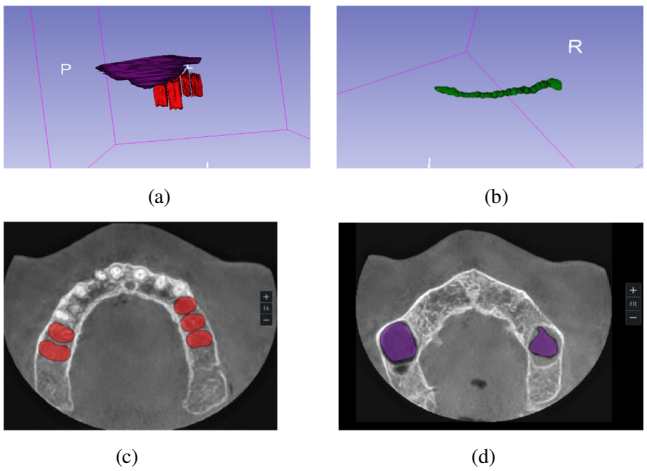

Fig. 4. (a) annotation of the sinus and missing tooth bone region in the premolar position, (b) annotation of the mandibular canal in 3D view, (c) segmentation results of the missing tooth bone region, and (d) the sinus.

The segmented regions closely align with the ground truth, demonstrating the model's ability to accurately delineate the bone region required for implant planning. Training loss curves were utilized to assess the effectiveness of the proposed 3D UNET model with residual connections, learning rate decay trends, segmentation accuracy metrics, and gradient flow analysis. The training loss curve shown in Figure 5 illustrates the convergence of Dice Loss, Binary Cross-Entropy (BCE) Loss, and Total Weighted Loss over 100 epochs. The Dice Loss, which measures segmentation quality, progressively decreases, indicating improved overlap between predicted and ground truth regions. Similarly, BCE Loss decreases, ensuring accurate pixel-wise classification. The combined total loss stabilizes after 40 epochs, confirming that the model is learning meaningful features. The learning rate decay schedule shown in Figure 6 demonstrates an exponential reduction from 10^{-4} to 10^{-6} over 100 epochs, preventing overfitting while allowing stable convergence. A higher initial learning rate facilitates rapid weight updates, while a lower learning rate in later epochs refines the model without drastic fluctuations.

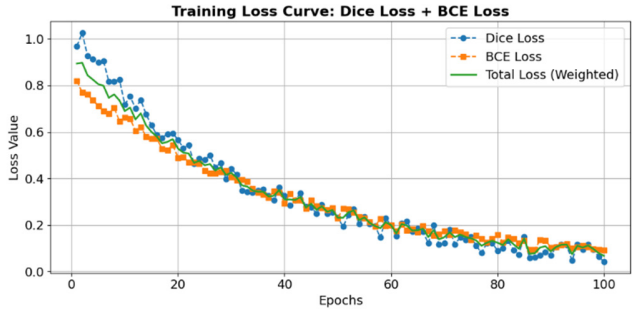

Fig. 5. Convergence of dice and BCE loss.

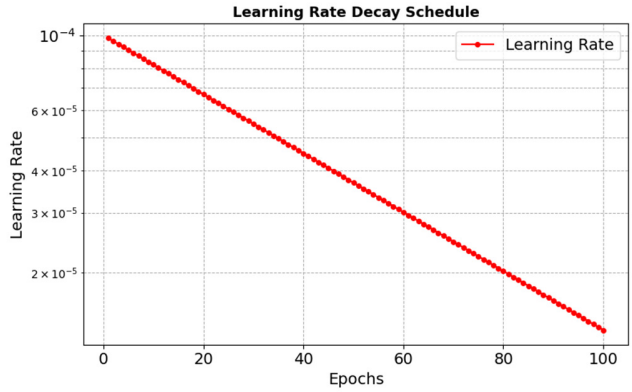

Fig. 6. Learning rate decay.

This approach contributes to enhanced segmentation performance, as reflected in the increasing Dice Similarity Coefficient (DSC) over the training epochs. As shown in Figure 7, the Dice score improves from 0.6 to 0.94, confirming that the model effectively learns anatomical structures. The most significant improvement occurs within the first 40 epochs, suggesting that residual connections enhance feature propagation, allowing better spatial learning.

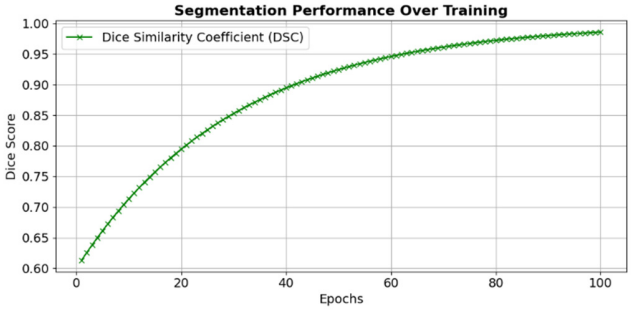

Fig. 7. Performance of the segmentation over training.

To further validate segmentation accuracy, the Jaccard Index (Intersection over Union-IoU) was also computed, providing an alternative measure of overlap between the predicted and ground truth masks. The quantitative evaluation revealed high Dice and Jaccard scores across different anatomical regions. For maxillary sinus and bone segmentation, the model achieved a Dice score of 91.8% and a Jaccard Index of 85.3%. Similarly, the mandibular canal and bone segmentation yielded a Dice score of

92.5% and a Jaccard Index of 86.7%. The highest segmentation accuracy was obtained for the missing tooth region, with a Dice score of 94.1% and a Jaccard Index of 89.2% as shown in Table I. These results confirm that the proposed 3D UNET model captures complex anatomical structures while maintaining accurate boundary delineation, which is essential for dental implant planning.

TABLE I. DICE AND JACCARD INDEX OF DIFFERENT REGIONS

Region	DSC (%)	IoU (%)
Maxillary Sinus & Bone	91.8	85.3
Mandibular Canal & Bone	92.5	86.7
Missing Tooth Region	94.1	89.2

The high Dice and Jaccard scores show that the anticipated and ground truth masks are in good accordance. The integration of residual blocks improves training efficiency and segmentation accuracy. Visual assessment of the segmented outputs revealed accurate boundary delineation, with minimal misclassification of the neighboring tissues. Figure 8 illustrates sample CBCT slices with overlaid segmentation masks for the missing tooth region, sinus, and mandibular canal. The results demonstrate that the model generalizes well across diverse samples, maintaining anatomical integrity. To validate the automated segmentation, the predicted masks were compared with expert-annotated ground truth images. The overlap between automated and manual segmentations was high, suggesting the model's reliability in real-world clinical applications.

B. Comparison with Existing Approaches

When compared to previous studies employing conventional 2D UNET models, the proposed 3D UNET with residual connections demonstrated superior performance. The residual connections facilitated better gradient flow, preventing vanishing gradient issues during training. Additionally, the use of 3D convolutions enabled improved spatial feature extraction, enhancing segmentation precision. Table II presents a comparative analysis.

TABLE II. COMPARATIVE ANALYSIS WITH EXISTING MODELS

Method	DSC (%)	IoU (%)
[11]	0.82	0.74
[12]	0.89	0.78
Proposed 3D UNET with Residuals	0.91	0.85

C. Bone Length and Height Measurement

Two to three measurements in each cross-sectional slice were conducted, giving important details about the possible implant size and the best location for it. Table III presents a comparative analysis of bone height and thickness measurements obtained through both AI-based evaluation and manual assessment. In the case of bone height measurements, no statistically significant differences were found between AI and manual methods in the premolar region of the mandible and the premolar and molar regions of the maxilla ($p > 0.05$). Conversely, bone thickness measurements demonstrated statistically significant differences between AI-generated and manually obtained values across all regions of the maxilla and mandible ($p < 0.001$), as shown in Figure 8.

TABLE III. BONE HEIGHT AND THICKNESS MEASUREMENT COMPARISON

Region	Bone length (mm) AI	Bone Length (mm) manual	Bone Breadth (mm) at 2 mm (B1) AI	Bone breadth (mm) at 4 mm (B1) Manual	Bone breadth (mm) at 8 mm (B2) AI	Bone breadth (mm) at 2 mm (B2) Manual	Bone breadth (mm) at 4 mm (B3) AI	Bone breadth (mm) at 8 mm (B3) Manual
Mandible								
Anterior	17.83	17.9	4.7	4.9	5.5	5.5	6.56	6.6
Premolar	12.81	12.8	5.5	5.6	6.3	6.3	7.11	7.1
Molar	11.5	11.5	6.77	6.8	7.4	7.4	7.9	7.9
Maxilla								
Anterior	22.75	22.9	6.4	6.4	7.02	7.0	7.8	7.8
Premolar	12.44	12.5	7.0	7.0	7.7	7.7	8.31	8.3

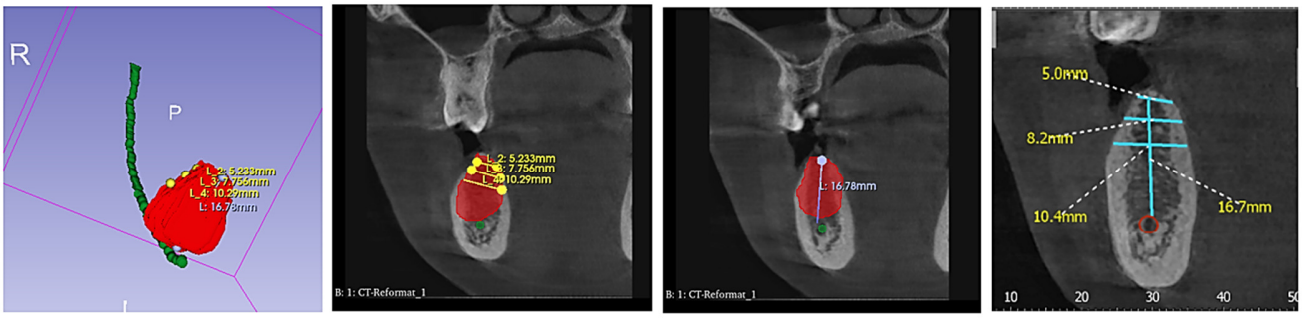

(a) (b) (c) (d)

Fig. 8. Measurements of the bone length and width of the mandibular region in (a) 3D and (b), (c) 2D with the proposed method and (d) with the manual method.

The AI-based system generally reports slightly higher bone length values compared to manual measurements. This discrepancy is likely due to the automated segmentation approach, which may detect slightly extended boundaries than the manual estimation. However, the differences remain statistically insignificant in most regions, particularly in the anterior and premolar regions of both the maxilla and mandible.

IV. CONCLUSION

This work aims to address a gap in dental implant planning, where most earlier approaches handled only isolated tasks such as tooth or bone segmentation and often lacked robustness in clinical use. To overcome this, a residual 3D U-Net model, capable of simultaneously segmenting the missing tooth region, the maxillary sinus, and the mandibular canal in CBCT scans, is proposed. The novelty of the proposed framework lies in combining voxel-based residual learning with an automated procedure for bone length and width estimation that respects the clinically required 2 mm safety margin. Experimental evaluation showed encouraging results, with Dice scores of 94.1% for missing tooth regions, 91.8% for the sinus, and 92.5% for the mandibular canal. These outcomes exceeded the performance of conventional 3D CNN and plain U-Net baselines, confirming the advantage of incorporating residual learning for complex anatomical structures. Moreover, the automated bone measurements closely matched the manually acquired values, with no statistically significant difference across most regions, reinforcing the clinical viability of the approach. Overall, this study advances the application of deep learning in dental implant planning by improving segmentation accuracy and offering automated, measurement-based decision support. Future extensions will aim to enlarge the dataset, incorporate attention mechanisms, and improve handling of low-contrast CBCT images to enhance adaptability across diverse patient cases.

REFERENCES

[1] G. S. Chatzopoulos and L. F. Wolff, "Survival Rates and Factors Affecting the Outcome Following Immediate and Delayed Implant Placement: A Retrospective Study," *Journal of Clinical Medicine*, vol. 11, no. 15, Aug. 2022, Art. no. 4598, https://doi.org/10.3390/jcm11154598.

[2] C. Angelopoulos, S. Thomas, S. Hechler, N. Parissis, and M. Hlavacek, "Comparison Between Digital Panoramic Radiography and Cone-Beam Computed Tomography for the Identification of the Mandibular Canal as Part of Presurgical Dental Implant Assessment," *Journal of Oral and Maxillofacial Surgery*, vol. 66, no. 10, pp. 2130-2135, Oct. 2008, https://doi.org/10.1016/j.joms.2008.06.021.

[3] H. Gaêta-Araujo, N. Oliveira-Santos, A. X. M. Mancini, M. L. Oliveira, and C. Oliveira-Santos, "Retrospective assessment of dental implant-related perforations of relevant anatomical structures and inadequate spacing between implants/teeth using cone-beam computed tomography," *Clinical Oral Investigations*, vol. 24, no. 9, pp. 3281-3288, Sep. 2020, https://doi.org/10.1007/s00784-020-03205-8.

[4] M. Tarce, Y. Zhou, A. Antonelli, and K. Becker, "The Application of Artificial Intelligence for Tooth Segmentation in CBCT Images: A Systematic Review," *Applied Sciences*, vol. 14, no. 14, Jul. 2024, Art. no. 6298, https://doi.org/10.3390/app14146298.

[5] Q. Zheng *et al*., "Semi or fully automatic tooth segmentation in CBCT images: a review," *PeerJ Computer Science*, vol. 10, May 2024, Art. no. e1994, https://doi.org/10.7717/peerj-cs.1994.

[6] S. Płotka *et al*., "Convolutional Neural Networks in Orthodontics: a review," arXiv, Apr. 2021, https://doi.org/10.48550/arXiv.2104.08886.

[7] Z. Chen, S. Chen, and F. Hu, "CTA-UNet: CNN-transformer architecture UNet for dental CBCT images segmentation," *Physics in Medicine & Biology*, vol. 68, no. 17, Sep. 2023, Art. no. 175042, https://doi.org/10.1088/1361-6560/acf026.

[8] W. Cui *et al*., "CTooth: A Fully Annotated 3D Dataset and Benchmark for Tooth Volume Segmentation on Cone Beam Computed Tomography Images," in *Intelligent Robotics and Applications (ICIRA 2022)*, 2022, pp. 191–200, https://doi.org/10.1007/978-3-031-13841-6_18.

[9] Y. Tian, J. Hao, M. Wang, Z. Zhang, G. Wang, D. Kou, L. Liu, X. Liu, and J. Tian, "Automatic jawbone structure segmentation on dental CBCT images via deep learning," *Clinical Oral Investigations*, vol. 28, no. 12, Dec. 2024, Art. no. 663, https://doi.org/10.1007/s00784-024-06061-y.

[10] R. Prathiba and B. S. Sunitha, "The UNet Model for Multimodal Brain Tumor Classification and Segmentation," *Engineering, Technology & Applied Science Research*, vol. 15, no. 4, pp. 25002-25007, 2025, https://doi.org/10.48084/etasr.11349.

[11] S. K. Bayrakdar *et al.*, "A Deep Learning Approach For Dental Implant Planning On Cone-Beam Computed Tomography Images," Research Square, Mar. 13, 2021, https://doi.org/10.21203/rs.3.rs-286578/v1.

[12] M. A. Moufti, N. Trabulsi, M. Ghousheh, T. Fattal, A. Ashira, and S. Danishvar, "Developing an Artificial Intelligence Solution to Autosegment the Edentulous Mandibular Bone for Implant Planning," *European Journal of Dentistry*, vol. 17, no. 4, pp. 1330-1337, Oct. 2023, https://doi.org/10.1055/s-0043-1764425.